

A structural study of bis-(trimethylamine)alane, $\text{AlH}_3 \cdot 2\text{NMe}_3$, by variable temperature X-ray crystallography and DFT calculations

Terry D. Humphries, Peter Sirsch, Andreas Decken, G. Sean McGrady *

Department of Chemistry, University of New Brunswick, P.O. Box 4400, Fredericton, NB, Canada E3B 5A3

ARTICLE INFO

Article history:

Received 5 November 2008
Received in revised form 3 December 2008
Accepted 3 December 2008
Available online 16 December 2008

Keywords:

Bis-(trimethylamine)alane
Alane
X-ray crystallography
DSC
DFT calculations
NMR spectroscopy

ABSTRACT

The structure of $\text{AlH}_3 \cdot 2\text{NMe}_3$ has been investigated by single-crystal X-ray diffraction over the range of 296–173 K. Over this temperature range a phase change is observed from *Cmca* to *Pbcm* where the methyl groups convert from a statistically disordered conformation to a mutually eclipsed conformation at lower temperatures. Measurement of the unit cell dimensions shows a decrease in the lengths of the **a** and **b** axes, and an increase in that of the **c** axis as the temperature is lowered, with inflections apparent between 223 and 233 K in the region of the phase change. Low-temperature DSC measurements reveal the change from *Pbcm* to *Cmca* to occur at 218.3 K, with an enthalpy of 107.7 J mol^{-1} . The molecular structure of $\text{AlH}_3 \cdot 2\text{NMe}_3$ is compared with those of related amine adducts of Group 13 hydrides, either measured experimentally or calculated using DFT methods. ^1H , ^{13}C and ^{27}Al NMR spectroscopy has also been utilized to characterize $\text{AlH}_3 \cdot 2\text{NMe}_3$ and its 1:1 counterpart $\text{AlH}_3 \cdot \text{NMe}_3$.

© 2009 Elsevier B.V. All rights reserved.

1. Introduction

The binary hydride of aluminum, AlH_3 or alane, is a sterically and electronically unsaturated moiety that reacts readily with a range of Lewis donors, leading to 1:1 and 1:2 adducts which are four- or five-coordinate at the Al centre, respectively [1–3]. A wide range of such adducts has been synthesized and characterized over the past 60 years, with donors including carbenes [4–6], phosphines [6–8], amines [9–12], ethers [13–15] and other O-derived functionalities [16].

Amongst these different types of alane adducts, amine complexes are the most widely studied and reported. The simplest amine adducts; viz. $\text{AlH}_3 \cdot \text{NMe}_3$ and $\text{AlH}_3 \cdot 2\text{NMe}_3$, were originally reported in 1942 by Wiberg and Stecher [9–11]. For the 1:2 adduct, Wiberg postulated a trigonal bipyramidal (TBP) structure, a prediction that was confirmed by Heitsch et al. in 1963 through a single-crystal X-ray structure determination at room temperature [17]. Heitsch et al. concluded that the complex indeed adopts a TBP structure, with axial amines and equatorial hydrogen ligands, and crystallizes in an orthorhombic space group *Cmca*, with unit cell parameters $a = 10.10 \text{ \AA}$, $b = 8.84 \text{ \AA}$, and $c = 12.94 \text{ \AA}$. Somewhat surprisingly, these authors also reported a dipole moment for the molecule in solution. The molecular structure was corroborated in the same year by Fraser et al., who measured the gas phase IR spectrum of $\text{AlH}_3 \cdot 2\text{NMe}_3$, and interpreted it in terms of a molecule

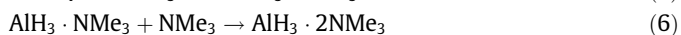
with D_{3h} symmetry. These authors also concluded that the molecule undergoes partial dissociation in the gas phase, in an equilibrium between the 1:2 and 1:1 adducts and free NMe_3 [18]. A subsequent gas electron diffraction (GED) study by Mastryukov et al. confirmed the D_{3h} molecular structure [19]; this study made allowance for the equilibrium described by Fraser et al., but found no significant amounts of $\text{AlH}_3 \cdot \text{NMe}_3$ or free NMe_3 in the GED pattern. The X-ray crystal structure of $\text{AlH}_3 \cdot \text{NMe}_3$ was reported by Raston et al., who found the compound to be dimeric in the solid state, as postulated by Wiberg [11]. In the gas phase the molecule is monomeric [20]. Other 1:1 alane complexes associate through unsymmetrical bridging hydrides in the crystalline state include the adducts with THF [16], $\text{NMe}_2(\text{CH}_2\text{Ph})$, 1-methyltetrahydropyridine [21] and $\text{NMe}_2(\text{CH}_2)_3\text{Cl}$ [22].

The preparation of $\text{AlH}_3 \cdot 2\text{NMe}_3$ is straightforward, and can be achieved by several routes. The original Wiberg synthesis involved the production of AlH_3 in Et_2O , followed by displacement of the ether ligand by the more basic Me_3N (Eqs. (1) and (2)) [9,10]. Heitsch et al. used a similar approach, substituting H_2SO_4 in place of HCl in the first step (Eqs. (3) and 4) [17]. More recently, Ruff and Hawthorne adopted the direct reaction between LiAlH_4 and Me_3NHCl in Et_2O , thereby employing the ammonium hydrochloride salt as the source of both acid and amine ligand in a single step to form the 1:1 complex (Eq. (5)) [23]. Excess NMe_3 must be condensed onto the amine–alane before sublimation to ensure complete production of the 1:2 complex (Eq. (6)). This route was previously employed by Schaeffer for the synthesis of $\text{BH}_3 \cdot \text{NMe}_3$ using LiBH_4 and $\text{NMe}_3 \cdot \text{HCl}$ [24]. The procedures for preparing the

* Corresponding author.

E-mail address: smcgrady@unb.ca (G.S. McGrady).

1:1 and 1:2 adducts are almost identical, except that the latter requires addition of an excess of NMe₃ prior to sublimation to guard against dissociation to the 1:1 complex.



The 1:1 and 1:2 adducts are white, air-sensitive crystalline materials that sublime readily at ambient temperature, and which as described above exist in equilibrium in the gas phase [18,25,26]. Under thermolysis, they decompose readily into crystalline Al, and Me₃N and H₂ gases [9]. The availability of high purity Al in this manner has prompted a large body of research into the use of these adducts in various types of methods of chemical vapour deposition (CVD) to produce Al thin films [27–29].

In the solid state, AlH₃·2NMe₃ is known to crystallize in at least two phases. In their earlier X-ray diffraction study, Heitsch et al. reported the existence of a phase change at –35 °C [17]. In this paper, we report an improved room temperature crystal structure for AlH₃·2NMe₃, a determination of the low temperature structure for the first time, and characterization of the phase transition between them by low-temperature DSC. In addition, variable temperature single-crystal X-ray diffraction has been conducted between –100 °C and room temperature in 10 °C increments, permitting us to monitor the temperature dependence of the crystal and molecular structure of AlH₃·2NMe₃. Finally, the ¹H, ¹³C and ²⁷Al NMR data for AlH₃·2NMe₃ are reported and compared with the corresponding values for the 1:1 adduct AlH₃·NMe₃.

2. Experimental

2.1. General considerations

All manipulations were performed using standard Schlenk or dry-box techniques in vacuo or under an atmosphere of purified nitrogen or argon (H₂O and O₂ < 1 ppm). Solvents were dried and deoxygenated using a Grubbs-type solvent dispensing system, degassed prior to use, and stored under argon. All starting materials were reagent grade from Sigma–Aldrich and were used as received, with the exception of LiAlH₄, which was purified by recrystallization from THF. The NMR spectra for AlH₃·NMe₃ and AlH₃·2NMe₃ were recorded in toluene-*d*₈. ¹³C spectra for both complexes and the ¹H spectrum for AlH₃·NMe₃ were measured using a Varian 300 NMR spectrometer. ²⁷Al spectra for both complexes and the ¹H spectrum for AlH₃·2NMe₃ were recorded using a Varian 400 spectrometer. ¹³C NMR spectra were referenced to the toluene-*d*₈ singlet at 137.86 ppm and ¹H spectra were referenced to the H NMR were referenced to the toluene-*d*₈ singlet at 7.09 ppm. ²⁷Al NMR were referenced using Al(NO₃)₃ in D₂O (1.1 mol/L) as an external standard. DSC measurements were conducted using a TA Instruments DSC Q200 with Perkin-Elmer Volatile Aluminum pans. The purge gas was UHP 5.0 He at 25 mL/min. Data were collected at 0.1 s/point. The method used included a temperature equilibration at –100 °C, isothermal for 1 min, followed by a temperature ramp of 2 °C/min to 400 °C.

2.2. Syntheses

2.2.1. AlH₃·2NMe₃

2.2.1.1. Method A. A preliminary qualitative reaction was conducted using a solution of AlH₃ prepared as described by Brown

and Yoon [30]. THF (50 mL) was added to purified LiAlH₄ (1.5 g; 40 mmol), and left to stir overnight. The suspension was cooled in an ice bath whilst conc. H₂SO₄ (2.0 g; 20 mmol) was added dropwise. A white precipitate of Li₂SO₄ quickly formed and H₂ evolution was apparent. The reaction mixture was stirred for 6 h and left to stand overnight, allowing the precipitate to settle. The supernatant solution was then filtered into a Schlenk tube. The concentration of the resulting AlH₃ solution was ca. 0.8 M. A 10 mL aliquot of this solution was transferred into an H-tube equipped with a magnetic stirrer flea and a coarse sintered glass frit between the two limbs. The vessel was cooled to –196 °C and partially evacuated, and gaseous Me₃N (9.0 g; 150 mol) was condensed on top of the frozen solution. Upon warming, the solution melted and a white precipitate was observed. The whole procedure was repeated one more time to ensure complete reaction, then the THF solution was transferred via cannula into a separate Schlenk flask and the THF was removed in vacuo, leaving a white powder on the bottom and colourless, irregular shaped crystals that had sublimed on the side of the flask. The remaining white powder in the H-tube was dissolved in toluene and washed through the frit: this solution deposited cubic crystals that decomposed rapidly on exposure to air.

2.2.1.2. Method B. LiAlH₄ (2.2 g; 58 mmol) and Me₃NHCl (4.5 g; 47 mmol) were introduced into a Schlenk flask, which was then cooled to –78 °C. Et₂O (100 mL) was added, and the contents were stirred and allowed to warm to room temperature. After 1 h, the solvent was then removed in vacuo, leaving a pasty white residue. To guarantee the 2:1 complex, NMe₃ gas was condensed into the flask and the contents were allowed to stir for 20 min. The flask was then warmed to 50 °C, and the contents sublimed into a separate flask cooled to –78 °C. A white crystalline powder thus obtained was stored at –37 °C in a glove box.

Yield: 3.4 g (98%). ¹H NMR (toluene-*d*₈): δ (ppm) = 3.42 (br, 3H, AlH₃), 2.13 (s, 18H; CH₃). ²⁷Al NMR (toluene-*d*₈): δ (ppm) = 111.49. ¹³C NMR (toluene-*d*₈): δ (ppm) = 47.39 (N–CH₃). The unit cell was measured by single-crystal X-ray diffraction, which confirmed the material as AlH₃·2NMe₃.

2.2.2. AlH₃·NMe₃

AlCl₃ (3.78 g, 28 mmol) and LiAlH₄ (3.69 g, 97 mmol) were introduced into an H-tube whose two limbs were separated by a sintered glass frit. The apparatus was cooled in an ice bath and pentane (100 mL) was added. NMe₃ (9 g; 152 mmol) was condensed onto the slurry, which was then allowed to warm to room temperature and stirred overnight. The resulting solution was filtered through the frit and the vessel was stored at –40 °C for 24 h, to afford a white crystalline powder. The pentane solvent was removed in vacuo, leaving a pasty white residue. The flask was then warmed to 50 °C, and the contents sublimed into a collection vessel cooled to –78 °C. The white powder thus obtained was stored at –37 °C in a glove box.

Yield: 1.092 g (10.8%). ¹H NMR; δ (ppm) = 3.92 (br, 3H, AlH₃), 1.89 (s, 9H; CH₃). ²⁷Al NMR; δ (ppm) = 139.81. ¹³C NMR; δ (ppm) = 47.76 (CH₃).

2.3. X-ray crystal structure determinations

Crystals of AlH₃·2NMe₃ were grown by sublimation in vacuo at room temperature. A suitable single crystal of dimensions (mm) 0.60 × 0.50 × 0.40 was selected in a glovebox, fixed in a glass capillary without oil and mounted on a Bruker AXS P4/SMART 1000 diffractometer. A hemisphere of data was collected using graphite monochromated Mo-Kα radiation (λ = 0.71073 Å) and ω- and θ-scans with a scan width of 0.3°. The unit cell parameters were obtained by least-squares refinement of 4579 reflections (low-temperature study at 173 K, LT) and 1780 reflections

Table 1
Crystallographic data for $\text{AlH}_3 \cdot 2\text{NMe}_3$.

	$T = 296(1) \text{ K}$	$T = 173(2) \text{ K}$
Chemical formula	$\text{C}_6\text{H}_{21}\text{AlN}_2$	$\text{C}_6\text{H}_{21}\text{AlN}_2$
M_r	148.23	148.23
Space group	<i>Cmca</i>	<i>Pbcm</i>
$a/\text{\AA}$	10.091(3)	8.462(2)
$b/\text{\AA}$	8.858(3)	13.412(3)
$c/\text{\AA}$	12.938(4)	9.640(2)
$\alpha/^\circ$	90	90
$\beta/^\circ$	90	90
$\gamma/^\circ$	90	90
$V/\text{\AA}^3$	1156.3(6)	1094.2(5)
Z	4	4
$F(000)$	336	336
$D_c/\text{g cm}^{-3}$	0.851	0.900
μ/mm^{-1}	0.121	0.128
$R_1^a(\text{obsd})$, $wR_2^b(\text{all})$	0.0501, 0.1816	0.0332, 0.0986
S^c	1.068	1.129
$R_{\text{int}}^d(\text{all equivalents})$	0.0178	0.0264

$$^a R_1 = \frac{\sum(|F_o| - |F_c|)}{\sum|F_o|}$$

$$^b wR_2 = \left\{ \frac{\sum[w(F_o^2 - F_c^2)]^2}{\sum[w(F_o^2)]^2} \right\}^{1/2}$$

$$^c S = \left[\frac{\sum w(F_o^2 - F_c^2)^2}{(n_o - n_p)} \right]^{1/2}$$

(room-temperature study at 296 K, RT) and a total number of 7161 (LT) and 3760 (RT) reflections were integrated, 1311 (LT) and 699 (RT) of which were unique [$R_{\text{int}} = 0.0264$ (LT), 0.0178 (RT)]. Raw data were integrated with the program SAINT [31] and corrections for absorption effects were applied using SADABS [32]. The structure was solved by a combination of direct methods (SHELXS) [33] and iterative difference-Fourier syntheses (SHELXTL) [34]. All non-hydrogen atoms were refined using anisotropic displacement parameters. For the room temperature study, hydride atoms were refined using isotropic displacement parameters; methyl hydrogen atoms were included in calculated positions and refined using a riding model. All hydride atoms and methyl groups were disordered over two positions. For the low-temperature study, all hydrogen atoms were refined using isotropic displacement parameters. The number of refined parameters was 94 (LT) and 50 (RT). The maximum residual electron density was 0.39 (LT) and 0.18 (RT) and minimum -0.11 (LT) and $-0.09 \text{ e}\text{\AA}^{-3}$ (RT). Further details of the refinement and crystallographic data are presented in Table 1. Plots were generated using the programs ORTEP-3 [35] and PLATON [36]. CCDC 705484 and 705485 contain the supplementary crystallographic data for this paper. These data can be obtained free of charge via www.ccdc.cam.ac.uk/conts/retrieving.html (or from the Cambridge Crystallographic Data Centre, 12, Union Road, Cambridge CB2 1EZ, UK; fax: +44 1223 336033).

The low-temperature (173 K) data were collected first. The crystal was then allowed to warm to room temperature (296 K) where a second data set was recorded. The variable temperature study was then conducted with the next data set being recorded at 249 K. Data were then collected in 10 K decrements with a 20 min period allowed for equilibration. A total of 120 frames were collected at each temperature enabling a unit cell to be determined. After the final measurement, the crystal was allowed to warm to room temperature and the unit cell was determined a final time to confirm that the structure had reverted to the space group *Cmca*.

2.4. Computational details

DFT calculations were performed with the GAUSSIAN 03 program suite [37] using the B3LYP density functional [38–40], along with the implemented 6-311G(d,p) basis set [41–44]. All geometry optimizations were carried out in C_{3v} (1:1 trimethylamine adducts of B, Al and Ga) and D_{3h} symmetry (1:2 adducts of Al and Ga), respectively. The reported structures were found to

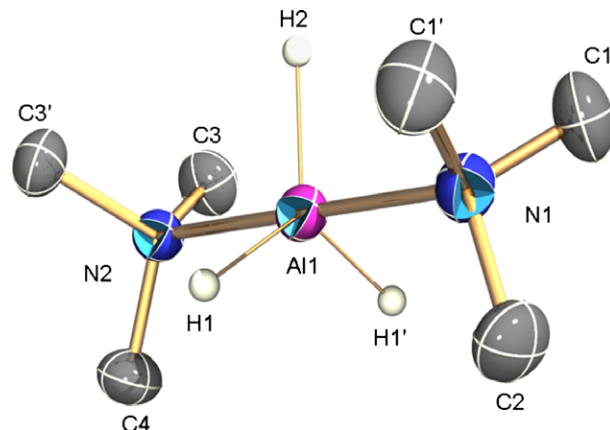


Fig. 1. Molecular structure of $\text{AlH}_3 \cdot 2\text{NMe}_3$ as determined by single-crystal X-ray diffraction at 173 K. All non-hydride hydrogen atoms are omitted for clarity and thermal ellipsoids are drawn at the 50% probability level. Selected bond lengths (\AA), angles ($^\circ$) and torsional angles ($^\circ$): Al–N1 2.163(2), Al–N2 2.163(2), Al–H1 1.55(2), Al–H2 1.52(2), N1–C1 1.471(2), N1–C2 1.470(2), N2–C3 1.472(2), N2–C4 1.470(2), N1–Al–N2 179.84(5), H1–Al–H2 120.7(5), H1–Al–N1 90.0(5), H2–Al–N1 90.2(7), Al–N1–C1 109.82(8), Al–N1–C2 109.0(2), C1–N1–C2 109.3(2), C2–N1–Al–H2 180, C4–N2–Al–H2 180, C2–N1–Al–H1 $-59.3(5)$.

be true minima on the potential energy surface by calculating analytical frequencies.

3. Results and discussion

3.1. Molecular structure of $\text{AlH}_3 \cdot 2\text{NMe}_3$

Fig. 1 shows the molecular structure determined for $\text{AlH}_3 \cdot 2\text{NMe}_3$ at 173 K. The molecule adopts a regular TBP array, with three equatorial hydrides and two axial amine ligands, which adopt a staggered conformation with respect to the central AlH_3 moiety. Table 2 presents a comparison of the molecular dimensions measured by us at 296 and 173 K with those reported by Heitsch et al. at room temperature [17] and by Mastrykov in the gas phase at 323 K [19]. In the earlier X-ray study, the hydrogen atoms could not be located independently due to disorder. The molecular parameters deduced from all four experiments are in good agreement, confirming that the structures at room temperature and 173 K differs only by the increased symmetry at lower temperature (Section 3.2).

Table 3 allows comparison of the salient structural parameters we have determined for $\text{AlH}_3 \cdot 2\text{NMe}_3$ with those reported for the 1:1 trimethylamine adducts of boron, aluminum and gallium, as well as their DFT-calculated counterparts. Al is unique amongst this triad of Group 13 elements in forming a stable 1:2 adduct. Although the Ga analogue appears theoretically stable at the B3LYP/6-311G(d,p) level of theory [$d(\text{E}-\text{H}) = 1.587 \text{ \AA}$,

Table 2

Comparison of salient bond lengths (\AA) and angles ($^\circ$) for $\text{AlH}_3 \cdot 2\text{NMe}_3$ in solid and gas phases studied by X-ray diffraction, GED measurements and DFT calculations.

	X-ray ^a	X-ray (RT) ^b	X-ray (LT) ^b	GED ^c	DFT ^d
Al–N	2.18(1)	2.174(2)	2.163(2)	2.19(2)	2.248
N–C	1.48(3)	1.422(5)–1.548(6)	1.470(2)–1.472(2)	1.48(5)	1.474
Al–H	–	1.51(4)–1.56(4)	1.52(2), 1.55(2)	1.53(3)	1.616
Al–N–C	110(2)	104.1(2)–114.9(2)	109.0(2)–110.0(2)	106.5(8)	108.7
N–Al–H	–	84(2)–95(2)	89.7(7)–90.2(7)	–	90.0

^a [17].

^b This work, study at 296 K (RT) and 173 K (LT), respectively.

^c [19].

^d This work.

Table 3

Comparison of selected bond lengths (Å) and angles (°) for $\text{EH}_3\cdot\text{NMe}_3$ (E = Al, Ga, B) studied by various techniques.

		E–H	E–N	H–E–N
$\text{BH}_3\cdot\text{NMe}_3$	Exp. ^a	1.211(3)	1.637	105.32(16)
	DFT ^b	1.210	1.658	105.5
$\text{AlH}_3\cdot\text{NMe}_3$	Exp. ^c	1.560(11)	2.063(7)	104.3(11)
	DFT ^b	1.602	2.099	99.8
	DFT ^d	1.609	2.074	100.0
$\text{GaH}_3\cdot\text{NMe}_3$	Exp. ^e	1.511(1)	2.134(4)	99.3(8)
	Exp. ^f	1.51(6)	2.081(4)	97(2)
	DFT ^b	1.581	2.196	98.5

^a Microwave spectroscopy [45].

^b This work.

^c Microwave spectroscopy [20].

^d MP2(full)/6-31G(d) calculations [46].

^e GED [47].

^f X-ray diffraction [47].

$d(\text{E–N}) = 2.415 \text{ \AA}$, $(\text{H–E–N}) = 90.0^\circ$], no such complex has been reported so far. As can be seen in Table 3, the E–N bond distance in the 1:1 adducts increases by around 0.4 \AA on progressing from B to Al, but by less than 0.1 \AA between Al and Ga. This reflects the trend in atomic properties down Group 13, with Al and Ga each having covalent radii of around 1.22 \AA , significantly larger than B at about 0.84 \AA [48]. The experimental and calculated E–N bond distances for the 1:2 adducts of Al (Table 2) and Ga (*op. cit.*) are about 10% longer than the corresponding values in their 1:1 counterparts, reflecting the increase in coordination number from 4 to 5 at the metal centre. The experimental and theoretical E–H distances are

all typical for their respective Group 13 element E, with no significant differences evident between the 1:1 and 1:2 complexes in the cases of Al and Ga.

The computational values presented in Table 3 are gas phase values for the monomeric species. Although $\text{AlH}_3\cdot\text{NMe}_3$ is a dimer in the solid state [21], it is a monomer in the gas phase [47]. There is no experimental or computational evidence to suggest that any of the other species in Table 3 is associated in the gas phase. Both Ga and B have a stronger preference for 4-coordination than does Al [3].

3.2. Crystal packing of $\text{AlH}_3\cdot 2\text{NMe}_3$

Initial X-ray diffraction studies were conducted at 173 K. Analysis of the diffraction pattern indicated space group $Pbcm$, in contrast to the earlier room temperature study by Heitsch et al. ($Cmca$) [17]. However, subsequent measurements on the same crystal at room temperature revealed space group $Cmca$, confirming the original report and indicating a reversible phase change between these two temperatures. A herringbone structure is evident in both phases, indicating only a slight conformational change within the unit cell at the phase transition (Figs. 2 and 3). The molecules are orientated in the same direction in each case, and the unit cells differ only slightly in their dimensions. Heitsch et al. solved their room temperature structure using a disordered model corresponding to a superposition of two orientations, 180° apart, of the trimethylamine group, represented by a hexagon of six half-methyls. The room temperature (296 K) structure presented here confirms that the NMe_3 ligands are statistically disordered (Fig. 2). In contrast, the low temperature structure reveals a mutually eclipsed conformation

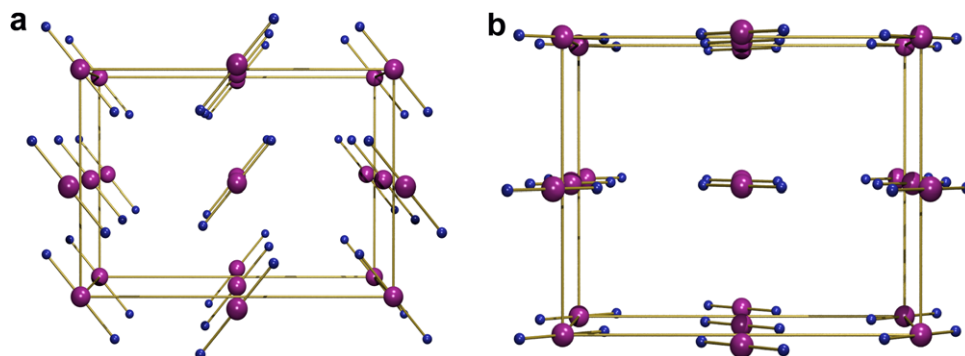


Fig. 2. Crystal packing of $\text{AlH}_3\cdot 2\text{NMe}_3$ at 296 K (space group $Cmca$). The methyl groups of the Me_3N moieties are disordered and omitted for clarity, as well as the hydrogen atoms bonded to Al. (a) View along **a** axis; (b) view along **b** axis.

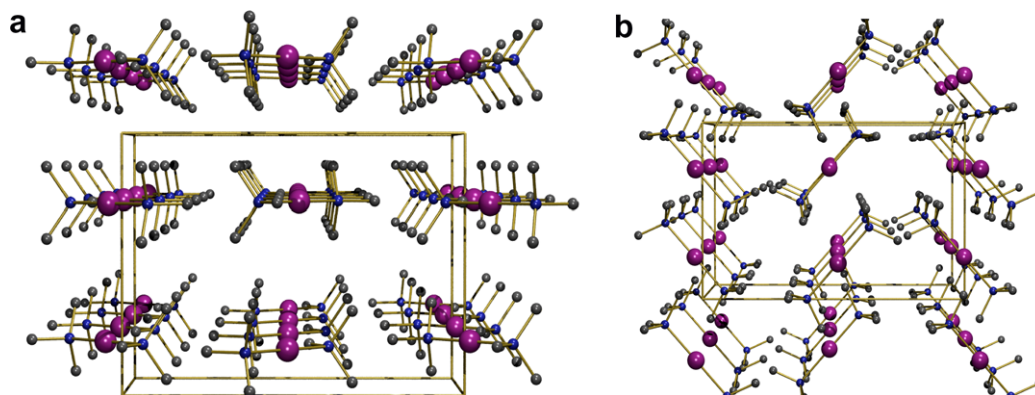


Fig. 3. Crystal packing of $\text{AlH}_3\cdot 2\text{NMe}_3$ at 173 K (space group $Pbcm$). Here the methyl groups of the Me_3N moieties exclusively adopt a staggered arrangement with respect to the central AlH_3 moiety. All hydrogen atoms are omitted for clarity. (a) View along **a** axis; (b) view along **c** axis.

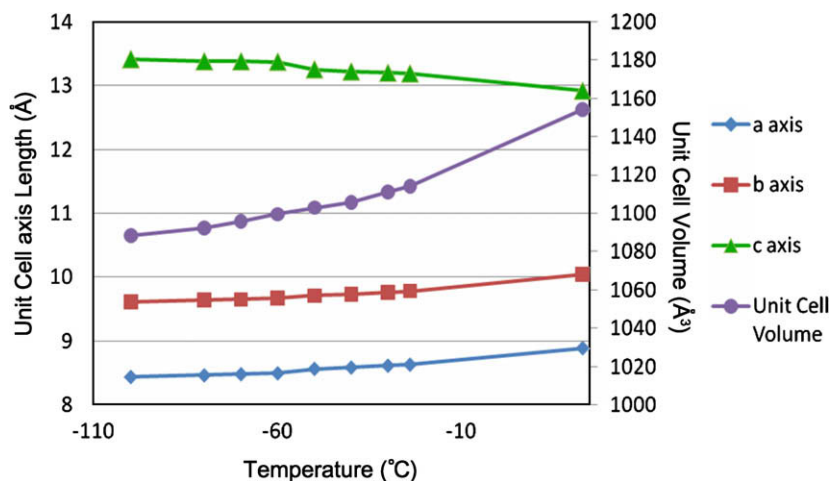


Fig. 4. Unit cell axis dimensions and cell volume as a function of temperature between +23 and -100 °C. Axes are labeled with respect to the structure at 296 K.

for the NMe_3 groups (Fig. 3), such that the methyl groups adopt a staggered arrangement with respect to the central AlH_3 moiety (see Fig. 1 for detail). The eclipsed conformation is preferred at low temperatures on account of its increased molecular symmetry and its correspondingly lower conformational entropy. As temperature increases, the molecules adopt a statically disordered conformation because of the higher entropy of this arrangement.

The molecular structure of $\text{AlH}_3 \cdot 2\text{NMe}_3$ determined from these experiments is discussed in Section 3.1. Closest intermolecular contacts in the crystal at 173 K were between $\text{Al}-\text{H} \cdots \text{H}-\text{C}$ with a distance of $2.58(3)$ Å and $\text{C}-\text{H} \cdots \text{H}-\text{C}$, at $2.60(2)$ Å. These distances are significantly longer than the sum of the van der Waals radii and give no indication for significant intermolecular interactions [49] or unconventional hydrogen bonding [50] between the molecules of $\text{AlH}_3 \cdot 2\text{NMe}_3$ in the solid state.

3.3. Variable temperature X-ray diffraction study of $\text{AlH}_3 \cdot 2\text{NMe}_3$

Upon lowering the temperature, the **a** and **b** axes of the unit cell were observed to contract while the **c** axis expanded; these two effects largely compensated for each other resulting in only a marginal decrease in the unit cell volume. The temperature dependence of these axes and the corresponding cell volume is depicted in Fig. 4, where an inflection can be seen for **a** and **c**

between -50 and -60 °C. This inflection corresponds to the change in space group from *Cmca* to *Pbcm*: as this change involves intramolecular adjustments of the orientation of the NMe_3 ligands with respect to each other, it has a barely discernible effect on the supramolecular structure and unit cell dimensions. Heitsch et al. [17] estimated the phase change to occur around -35 °C; however, our study places it around 20 °C lower than this value. The facile thermal cycling of the single crystal used in this study is likely assisted by the small changes in unit cell dimensions at the phase transition: a more discontinuous structural change would likely cause the crystal to fracture or deteriorate. Between -30 and -60 °C a significant amount of disorder is evident in the structure, which complicated the analysis of the data in terms of an orthorhombic unit cell. The disorder is due to the simultaneous presence of both high temperature and low temperature molecular conformations of $\text{AlH}_3 \cdot 2\text{NMe}_3$ within the crystal lattice over this temperature regime.

3.4. Low-temperature DSC study of $\text{AlH}_3 \cdot 2\text{NMe}_3$

In order to determine more precisely the temperature of the phase transition and to measure its enthalpy, low-temperature DSC experiments were carried out. At -54.82 °C, a small endothermic peak was observed in the trace, with an enthalpy of 107.7 J mol $^{-1}$ (Fig. 5). This corresponds to the transition from the *Pbcm* to *Cmca* structure, and the temperature measured for this transition corresponds well with the variable temperature X-ray data collected.

3.5. NMR spectroscopic study of $\text{AlH}_3 \cdot 2\text{NMe}_3$ and $\text{AlH}_3 \cdot \text{NMe}_3$

Surprisingly, no NMR spectroscopic characterization of $\text{AlH}_3 \cdot 2\text{NMe}_3$ appears to have been published; nor have ^{13}C and ^{27}Al NMR data been reported for $\text{AlH}_3 \cdot \text{NMe}_3$. Table 4 compares the ^1H , ^{13}C and ^{27}Al chemical shifts measured by us for $\text{AlH}_3 \cdot 2\text{NMe}_3$

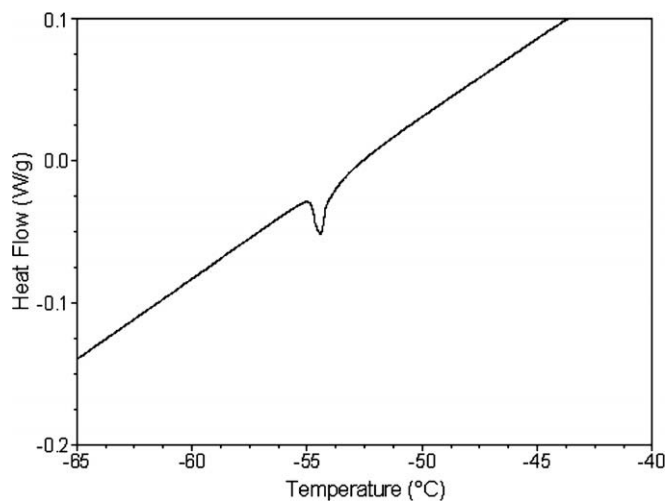


Fig. 5. Low-temperature DSC trace for a sample of $\text{AlH}_3 \cdot 2\text{NMe}_3$. The endothermic peak at -54.82 °C ($\Delta H = 107.7$ J mol $^{-1}$) corresponds to the phase change from *Pbcm* to *Cmca*.

Table 4
 ^1H , ^{13}C and ^{27}Al chemical shifts measured for $\text{AlH}_3 \cdot \text{NMe}_3$ and $\text{AlH}_3 \cdot 2\text{NMe}_3$.

	^1H		^{13}C	^{27}Al
	Al-H	C-H		
$\text{AlH}_3 \cdot \text{NMe}_3^a$	3.92	1.89	47.8	139.8
$\text{AlH}_3 \cdot \text{NMe}_3^b$	3.70	1.87	–	–
$\text{AlH}_3 \cdot 2\text{NMe}_3^a$	3.42	2.13	47.4	111.4

All chemical shifts reported in ppm.

^a This study (toluene- d_8).

^b [52] (Benzene d_6).

and $\text{AlH}_3\cdot\text{NMe}_3$. As would be expected, the corresponding features are quite similar. The hydride chemical shift for both the 1:1 and 2:1 complexes appears as a very broad singlet, on account of efficient relaxation by the quadrupolar ^{27}Al nucleus. This effect is more pronounced in the 2:1 complex; with its low symmetry TBP geometry at the Al nucleus the FWHM of 486 Hz is significantly larger than the corresponding value of 63 Hz for the 1:1 counterpart, which displays a *pseudo* tetrahedral environment at Al. In a similar vein, the ^{27}Al resonances of the 2:1 and 1:1 adducts have FWHM values of 1164 and 724 Hz, respectively. The additional amine ligand in the 2:1 complex causes the hydride ^1H and ^{27}Al resonances to appear at lower frequencies than in the 1:1 species, presumably on account of the increased electron density at the Al centre. These NMR spectral features are in general accord with those reported for other amine–alane complexes, such as $\text{AlH}_3\cdot\text{NMe}_2\text{Et}$ reported by Frigo et al. [51].

4. Conclusions

This study has improved on and extended the structural determination of $\text{AlH}_3\cdot 2\text{NMe}_3$ published by Heitsch et al. in 1963. We have confirmed and improved the *Cmca* room temperature structure in this earlier study. At ambient temperature, the orientation of the methyl groups in the $\text{Me}_3\text{N–Al–NMe}_3$ moiety is statistically disordered. As the temperature of the crystal is decreased, there is a phase change to *Pbcm* at around $-55\text{ }^\circ\text{C}$, which we have characterized independently by low-temperature DSC experiments. In the low temperature *Pbcm* phase, the orientation of the amine methyl groups in the $\text{Me}_3\text{N–Al–NMe}_3$ moiety is exclusively mutually eclipsed, which allows each NMe_3 group to adopt a staggered arrangement with the planar central AlH_3 unit. The NMR spectral characteristics of $\text{AlH}_3\cdot 2\text{NMe}_3$ and its 1:1 counterpart are reported and are in accord with those of related amine–alane complexes.

Acknowledgements

The authors would like to thank Keelie Munroe for assistance with the DFT calculations presented in Tables 2 and 3, Michael Johnson for the DSC measurements reported in Fig. 5 and Dr. Larry Calhoun for NMR spectroscopy assistance. We are grateful to NSERC and CFI for support of this work, and we thank the Atlantic Computational Excellence Network (ACEnet) for providing access to their computing facilities.

Appendix A. Supplementary data

Cartesian coordinates and geometrical parameters at the B3LYP/6-311G(d,p) level of theory for $\text{BH}_3\cdot\text{NMe}_3$, $\text{AlH}_3\cdot\text{NMe}_3$, $\text{AlH}_3\cdot 2\text{NMe}_3$, $\text{GaH}_3\cdot\text{NMe}_3$ and $\text{GaH}_3\cdot 2\text{NMe}_3$. Supplementary data associated with this article can be found, in the online version, at doi:10.1016/j.molstruc.2008.12.022.

References

[1] S. Cucinella, A. Mazzel, W. Marconi, *Inorg. Chim. Acta* 4 (1970) 51.
 [2] C. Jones, G.A. Koutsantonis, C.L. Raston, *Polyhedron* 12 (1993) 1829.
 [3] M.G. Gardiner, C.L. Raston, *Coord. Chem. Rev.* 166 (1997) 1.
 [4] M.D. Francis, D.E. Hibbs, M.B. Hursthouse, C. Jones, N.A. Smithies, *J. Chem. Soc. Dalton Trans.* (1998) 3249.

[5] A.J. Arduengo, H.V.R. Dias, J.C. Calabrese, F. Davidson, *J. Am. Chem. Soc.* 114 (1992) 9724.
 [6] J.L. Atwood, K.W. Butz, M.G. Gardiner, C. Jones, G.A. Koutsantonis, C.L. Raston, K.D. Robinson, *Inorg. Chem.* 32 (1993) 3482.
 [7] F.M. Elms, M.G. Gardiner, G.A. Koutsantonis, C.L. Raston, J.L. Atwood, K.D. Robinson, *J. Organomet. Chem.* 449 (1993) 45.
 [8] F.R. Bennett, F.M. Elms, M.G. Gardiner, G.A. Koutsantonis, C.L. Raston, N.K. Roberts, *Organometallics* 11 (1992) 1457.
 [9] O. Stecher, E. Wiberg, *Ber. Dtsch. Chem. Ges.* 75 (1942) 2003.
 [10] E. Wiberg, H. Graf, M. Schmidt, R. Uson, *Z. Naturforsch. B* 7 (1952) 578.
 [11] E. Wiberg, H. Graf, R. Uson, *Z. Anorg. Allg. Chem.* 272 (1953) 221.
 [12] C.J. Harlan, S.G. Bott, A.R. Barron, *J. Chem. Crystallogr.* 28 (1998) 649.
 [13] F.M. Brower, N.E. Matzek, P.F. Reigler, H.W. Rinn, C.B. Roberts, D.L. Schmidt, J.A. Snover, K. Terada, *J. Am. Chem. Soc.* 98 (1976) 2450.
 [14] G.K. Lund, J.M. Hanks, H.E. Johnston, *Production of α -alane*, 2007066839, 2007.
 [15] G.K. Lund, J.M. Hanks, H.E. Johnston, *Method for the production of α -alane*, 2005222445, 2005.
 [16] I.B. Gorrell, P.B. Hitchcock, J.D. Smith, *Chem. Commun.* (1993) 189.
 [17] C.W. Heitsch, R.W. Parry, C.E. Nordman, *Inorg. Chem.* 2 (1963) 508.
 [18] G.W. Fraser, B.P. Straughan, N.N. Greenwood, *J. Chem. Soc.* (1963) 3742.
 [19] V.S. Mastryukov, A.V. Golubinskii, L.V. Vilkov, *J. Struct. Chem.* 20 (1979) 788.
 [20] H.E. Warner, Y. Wang, C. Ward, C.W. Gillies, L. Interrante, *J. Phys. Chem.* 98 (1994) 12215.
 [21] F.M. Elms, C. Jones, C.L. Raston, K.D. Robinson, *J. Am. Chem. Soc.* 113 (1991) 8183.
 [22] P.C. Andrews, M.G. Gardiner, C.L. Raston, V.A. Tolhurst, *Inorg. Chim. Acta* 259 (1997) 249.
 [23] J.K. Ruff, M.F. Hawthorne, *J. Am. Chem. Soc.* 82 (1960) 2141.
 [24] G.W. Schaeffer, E.R. Anderson, *J. Am. Chem. Soc.* 71 (1949) 2143.
 [25] C.W. Heitsch, *Nature* 195 (1962) 995.
 [26] C.M.B. Marsh, H.F. Schaefer, *J. Phys. Chem.* 99 (1995) 195.
 [27] D.B. Beach, S.E. Blum, F.K. Legoues, *J. Vac. Sci. Technol. A* 7 (1989) 3117.
 [28] C. Popov, B. Ivanov, V. Shanov, *J. Appl. Phys.* 75 (1994) 3687.
 [29] T.H. Baum, C.E. Larson, *High Temp. Sci.* 27 (1989) 237.
 [30] H.C. Brown, N.M. Yoon, *J. Am. Chem. Soc.* 88 (1966) 1464.
 [31] SAINT 7.23A, Bruker AXS Inc., Madison, WI, USA, 2006.
 [32] G.M. Sheldrick, SADABS, Bruker AXS Inc., Madison, WI, USA, 2004.
 [33] G.M. Sheldrick, SHELXS, University of Göttingen, Germany, 2001.
 [34] G.M. Sheldrick, SHELXTL 6.14, Bruker AXS Inc., Madison, WI, USA, 2000.
 [35] L.J. Farrugia, *J. Appl. Crystallogr.* 30 (1997) 565.
 [36] A.L. Spek, *J. Appl. Crystallogr.* 36 (2003) 7.
 [37] M.J. Frisch, G.W. Trucks, H.B. Schlegel, G.E. Scuseria, M.A. Robb, J.R. Cheeseman, J.A. Montgomery, T. Vreven, K.N. Kudin, J.C. Burant, J.M. Millam, S.S. Iyengar, J. Tomasi, V. Barone, B. Mennucci, M. Cossi, G. Scalmani, N. Rega, G.A. Petersson, H. Nakatsuji, M. Hada, M. Ehara, K. Toyota, R. Fukuda, J. Hasegawa, M. Ishida, T. Nakajima, Y. Honda, O. Kitao, H. Nakai, M. Klene, X. Li, J.E. Knox, H.P. Hratchian, J.B. Cross, V. Bakken, C. Adamo, J. Jaramillo, R. Gomperts, R.E. Stratmann, O. Yazyev, A.J. Austin, R. Cammi, C. Pomelli, J.W. Ochterski, P.Y. Ayala, K. Morokuma, G.A. Voth, P. Salvador, J.J. Dannenberg, V.G. Zakrzewski, S. Dapprich, A.D. Daniels, M.C. Strain, O. Farkas, D.K. Malick, A.D. Rabuck, K. Raghavachari, J.B. Foresman, J.V. Ortiz, Q. Cui, A.G. Baboul, S. Clifford, J. Cioslowski, B.B. Stefanov, G. Liu, A. Liashenko, P. Piskorz, I. Komaromi, R.L. Martin, D.J. Fox, T. Keith, M.A. Al-Laham, C.Y. Peng, A. Nanayakkara, M. Challacombe, P.M.W. Gill, B. Johnson, W. Chen, M.W. Wong, C. Gonzalez, J.A. Pople, *Gaussian 03, Revision D.02*, Wallingford, CT, 2004.
 [38] A.D. Becke, *J. Chem. Phys.* 98 (1993) 5648.
 [39] C. Lee, W. Yang, R.G. Parr, *Phys. Rev. B* 37 (1988) 785.
 [40] B. Miehlich, A. Savin, H. Stoll, H. Preuss, *Chem. Phys. Lett.* 157 (1989) 200.
 [41] A.D. McLean, G.S. Chandler, *J. Chem. Phys.* 72 (1980) 5639.
 [42] R. Krishnan, J.S. Binkley, R. Seeger, J.A. Pople, *J. Chem. Phys.* 72 (1980) 650.
 [43] R.C. Binning Jr., L.A. Curtiss, *J. Comput. Chem.* 11 (1990) 1206.
 [44] L.A. Curtiss, M.P. McGrath, J.P. Blaudeau, N.E. Davis, R.C. Binning Jr., L. Radorn, *J. Chem. Phys.* 103 (1995) 6104.
 [45] J.R. Durig, Y.S. Li, J.D. Odom, *J. Mol. Struct.* 16 (1973) 443.
 [46] I. Abderrahim Boutalib, N.-G. Abdallah Jarid, F. Toms, *J. Phys. Chem. A* 105 (2001) 6526.
 [47] P.T. Brain, H.E. Brown, A.J. Downs, T.M. Greene, E. Johnsen, S. Parsons, D.W.H. Rankin, B.A. Smart, C.Y. Tang, *J. Chem. Soc. Dalton Trans.* (1998) 3685.
 [48] B. Cordero, V. Gomez, A.E. Platero-Prats, M. Reves, J. Echeverria, E. Cremades, F. Barragan, S. Alvarez, *J. Chem. Soc. Dalton Trans.* (2008) 2832.
 [49] A. Bondi, *J. Phys. Chem.* 68 (1964) 441.
 [50] T. Steiner, G.R. Desiraju, *Chem. Commun.* (1998) 891.
 [51] D.M. Frigo, G.J.M. Vaneijden, P.J. Reuvers, C.J. Smit, *Chem. Mater.* 6 (1994) 190.
 [52] D.G. Hendrick, C.W. Heitsch, *J. Phys. Chem.* 71 (1967) 2683.